Probing the E/K peptide coiled-coil assembly by double electron-electron resonance and circular dichroism

Elena A. Golysheva,[1] Aimee L. Boyle,[2] Barbara Biondi,[3] Paolo Ruzza,[3] Alexander Kros,[2] Jan Raap,[2*] Claudio Toniolo,[3] Fernando Formaggio,[3] Sergei A. Dzuba[1,4*]

[1] V.V. Voevodsky Institute of Chemical Kinetics and Combustion, Novosibirsk 630090, Russian Federation

[2] Leiden Institute of Chemistry, Gorlaeus Laboratories, Leiden University, 2300 RA Leiden, The Netherlands

[3] Institute of Biomolecular Chemistry, Padova Unit, CNR, 35131Padova, Italy; Department of Chemical Sciences, University of Padova, 35131 Padova, Italy

[4] Novosibirsk State University, Novosibirsk 630090, Russian Federation

1 Supporting Information

Email: J.Raap@chem.leidenuniv.nl

Dzuba@kinetics.nsc.ru

ABSTRACT: Double electron-electron resonance (DEER, also known as PELDOR) and circular dichroism (CD) spectroscopies were explored for studying the specificity of the conformation of peptides induced by their assembling into a self-recognizing system. For the pair of peptides (K and E) known to form a coiled-coil heterodimer, two paramagnetic TOAC α-amino acid residues were incorporated in each of the peptides (denoted as K** and E**) and a 3D-structural investigation with or without the presence of their unlabeled counterparts E and K was performed. The TOAC spin labels, replacing two Ala residues in each compound, are covalently and *quasi*-rigidly connected to the peptide backbone. They are known not to disturb the native peptide helical structure so that any conformational change can easily be monitored and assigned. DEER spectroscopy enables the measurement of intramolecular electron spin-spin distance distribution between the two TOAC labels, within the length of 1.5 – 8 nm. This method allows the individual conformational changes for the K**, K**/E, E**, and E**/K molecules to be investigated in glassy frozen solutions. Our data reveals that the conformations of the E** and K** peptides are strongly influenced by the presence of their counterparts. The results are discussed with those from CD spectroscopy and with reference to the already reported NMR data. It is concluded that the combined DEER/TOAC approach allows obtaining accurate and reliable information on the peptide conformation before and after their assembling to coiled-coil heterodimers. The potential applications of this method to other two-component, but more complex, systems, like receptor/antagonists, receptor/hormone, and enzyme/ligand, are discussed.

INTRODUCTION

The E and K peptides, named for the prevalence of Glu and Lys in their respective sequences, were designed to self-assemble into a heterodimeric coiled coil.[1] This intermolecular self-association motif has been used for a variety of applications, including labelling of membrane proteins in live cells,[2] as components of biosensors,[3] and as a membrane fusion system,[4-5] which has enabled the successful delivery of the anticancer drug doxorubicin to HeLa cells and to xenografted cells in zebrafish.[6]

The 3-heptad (21-amino acid) E/K coiled-coil system has been already studied under different conditions, *e.g.* the 3D-structure has been elucidated using 2D NMR,[7] paramagnetic NMR has been employed to probe peptide orientation and oligomer state,[8] and CD spectroscopy has provided information regarding the secondary structure in solution.[1]

The continuous-wave electron paramagnetic resonance (CW-EPR) technique was used to study peptide conformation with double spin-labeled peptide samples (at the $i + 4 \rightarrow i$ and $i + 3 \rightarrow i$ residue positions) to determine and distinguish α- and 3_{10}- helical conformations, which would be otherwise more difficult to identify only by CD and nuclear Overhauser enhancement NMR.[9] However, this EPR application requires multiple, different spin-labeled samples for providing enough conformational information on long, 3-heptad, (21-amino acid) peptide sequences.

DEER[10] is a sensitive method to investigate peptide conformation by measuring the electron dipole-dipole interactions of two intramolecularly positioned spin labels which enables electron spin-spin distance distribution within the length of 1.5 – 8 nm to be resolved. Recently, DEER has been used[11] for the 3D-structural investigation of the K/E coiled coil from *mono* MTSL[S-(1-oxyl-2,2,5,5-tetramethyl-2,5-dihydro-1H-pyrrol-3-yl)   methyl   methanesulfonothioate]-labeled K and E peptides, *i.e.* MTSL-C-K/E-C-MTSL (where C stands for Cys), with labels selectively situated at the N- and C-ends of either the K or the E peptide. The distances between the two nitroxide oxygen atoms were found to be in acceptable agreement with those reported

from the NMR structure. Also, the presence of K homo-dimers was observed from a sample of pure *mono* MTSL-labeled K (MTSL-C-K). MTSL labels can be rather easily introduced by reaction to the thiol group of a Cys residue, but at the risk of the accuracy of the acquired 3D-structural information due to the high flexibility of the MTSL-Cys side chain. Much more accurate results would be expected from measurements using the *quasi*-rigid 4-amino-1-oxyl-2,2,6,6-tetramethylpiperidine-4-carboxylic acid (TOAC) spin label. Note that the use of TOAC spin labelling in CW-EPR and DEER measurements has become a routine technique during the last decade.[12,13]

When applied to studying the peptide conformations, DEER spectroscopy, combined with intramolecularly *double*-labeled samples positioned at a long distance (~1.5 - 8 nm), provides a distance distribution function for the distance between the two labels which is directly related to one or more of the low-energy conformations seen in the peptide Ramachandran plot,[14] characterized by their typical ranges of the φ, ψ backbone torsion angles, *i.e.* α- (3.6_{13}), 3_{10}- (multiple β-turns), 2.2_{7}- (multiple γ-turns) helices, and the β-strand conformation. The length of the different conformations for a peptide with a given number of residues increases in the order α- < 3_{10}- < 2.2_{7}-helices< β-strand.[14,15] The key to this approach is that for a peptide segment of 21 residues, sufficient information can be obtained from a single double-labeled sample. The accuracy of the measurement mostly depends on the precise relative position of the nitroxide radicals. Therefore, the use of the *quasi*-rigid TOAC label is crucial for providing accurate results. Previously, the approach of double TOAC labeling has been reported for the DEER study of peptide conformations for membrane active antibiotic lipopeptides trichogin GA IV,[16-18] alameticin,[19] ampullosporin,[18] chalciporin A.[12a]

In contrast to previous studies of self-assembling peptides, in this paper we report on the conformation before and after assembling of the *two*-component self-recognizing coiled coil forming E and K peptides by measuring, *via* DEER, the induction of a helical conformation for

the [4,18] double TOAC-labeled peptides K and E (denoted as K** and E**, correspondingly) by its assembled unlabeled E counterpart, and *vice versa*. Distance distributions are obtained under different conditions, *i.e.* phosphate-buffered saline (PBS) (for comparison with the previously reported *mono*-MTSL labeled K and E peptides) and mixtures of PBS with 2,2,2-trifluoroethanol (TFE) (Table 1). The PBS/TFE mixtures are of interest because the NMR structure was resolved under similar conditions (23% TFE/PBS).[7] The 50% TFE/PBS mixture was used in the paramagnetic NMR analysis to show the disruption of the heterodimer,[8] and the 100% TFE condition for its well-known helix-inducing capability. The emerging conformational characteristics of the peptides are supported by those extracted from a CD investigation.

Table 1

Peptide sequences investigated (**T**=TOAC)	Abbreviation
Ac-(KIAALKE)$_3$-NH$_2$	K
Ac-(EIAALEK)$_3$-NH$_2$	E
Ac-KIA**T**LKE-KIAALKE-KIA**T**LKE-NH$_2$	K**
Ac-EIA**T**LEK-EIAALEK-EIA**T**LEK-NH$_2$	E**

The solution conditions used were selected for comparison with existing DEER or NMR literature data on the peptide structure: PBS with 20 % of glycerol added for glass formation upon freezing,[11] 20/80 (*v/v*) TFE/PBS mixture,[7] and 50/50 (*v/v*) TFE/PBS mixture.[8] Also, pure TFE was employed for conditions reflecting the expected full-helix propensity of the peptides.

This paper describes the DEER signal time traces and distance distributions for the K** and E** *bis*-labeled peptides, and their coiled coils K**/E and E**/K assemblies. The derived distance distributions agree very well with those expected for pure and rather rigid α-helices in glassy solutions. From the kinetics of the signal decay, it is found that K** forms self-assembling homodimers K**/K**, while this type of oligomerization is found to be prevented in the presence of unlabeled E, due to formation of coiled-coil heterodimers. The influence of TFE on peptide conformation is also discussed. Special attention is paid to the possible dependence of DEER data on both the mutual distance separation between two spin labels but also on their mutual orientation, the latter effect known as orientational selectivity.[20]

Taken together, the results obtained clearly show the potential of this combined DEER/TOAC approach in the investigation of the specificity of the conformation induced by peptide assembling into a self-recognizing system.

EXPERIMENTAL SECTION

Molecular Models

A molecular model of the spin-labeled analog of peptide K was derived using the HyperChem Professional 8.0 software (Hypercube, Inc.). The α-helical structure of the peptide was created by the 'built in' option in this package (φ and ψ torsion angles: 58°, 47°). TOAC residues were created from Ala^4 and Ala^{18}, followed by their geometric optimizations using the Allinger's molecular mechanics program of Hyperchem,[21] which is well-suited for the conformational optimization 5- and 6-membered homo- and hetero-cycloalkanes.[22]

Results of calculations are presented in Figure 1. The distance between the two nitroxide oxygen atoms of K** is calculated to be 2.1 nm, *i.e.* slightly overestimated because the maximum electron density of the unpaired electrons would be between the nitrogen and oxygen atoms. The distances shown in Figure 1 are calculated from the $C^α$-atoms of amino acid residues

by Hyperchem for a set of standard conformations. 'N' is the number of amino acid residues involved in the distance calculations. Torsion angles φ and ψ for these conformations used are: 58º, 47º (α), 49º, 28º (3_{10}), 75º, 70º (2_7), and 139º, 135º (β), respectively.[23]

The histograms regarding the NMR distance distribution shown in the abscissa of Figures 5 and 6 were derived from 20 models of the NMR E/K heterodimer 3D-structure. The distances were calculated from the coordinates of the C^α-atoms of the K- and E [Ala[4]] and K-[Ala[18]] residues which were taken from the PDB file 1UOL.[7] The helical wheel diagrams of the K**/K** and K**/E assemblies were prepared using DrawCoil, 1.0, from the Grigoryan Lab: https://grigoryanlab.org/drawcoil/
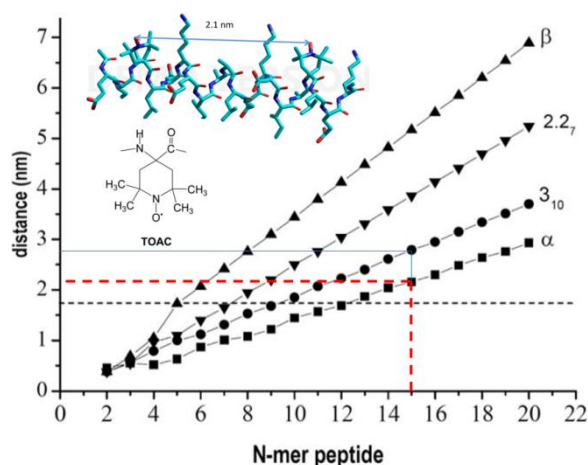

Figure 1. Distances between the C^α-atoms of the terminal residues of N-mer peptides calculated for standard α-, 3_{10}-, and 2.2_7- helices and the β-sheet conformation using the HyperChem Professional 8.0 software. DEER measurements of distances are reliable with an accuracy of +/- 0.03 nm) within the range of ≈ 1.5 to ≈ 8 nm (black dashed line). Insets: α-helix structure of the double nitroxide labeled [TOAC[4,18]]K**-peptide, TOAC chemical structure, and predicted distance between the free-radical oxygen atoms of the two TOAC residues (red dashed line).[13]

Peptide Synthesis and Characterization

Fmoc (9-fluorenylmethyloxycarbonyl)-amino acids were obtained from Iris-Biotech (Marktredwitz, Germany). All other protected amino acids and reagents for peptide synthesis were supplied by Sigma–Aldrich (St. Louis, MO).

The solid-phase peptide syntheses (SPPS) of the two *unlabeled* peptides were facilitated using a microwave-assisted Liberty Blue automated peptide synthesizer. Both peptides were synthesized on Tentagel HL RAM resin using standard Fmoc-chemistry protocols. N, N'-diisopropylcarbodiimide (DIC)/Oxyma Pure were employed as activator/base, respectively for the coupling steps. Once the automated synthesis was completed, the N-terminus of both peptides was manually acetylated using a mixture of acetic anhydride (Ac_2O) and pyridine in dimethylformamide (DMF). The resin was subsequently washed with DMF followed by dichloromethane (DCM), and the peptide was cleaved using a mixture of trifluoroacetic acid (TFA), triisopropylsilane (TIS), and water in the ratio: 95:2.5:2.5, (TFA:TIS:H_2O). The peptide was precipitated into ice-cold diethyl ether, collected by centrifugation, resuspended in a mixture of water and acetonitrile, and freeze-dried.

Assembly of the *TOAC-containing peptides* on the Biotage (Uppsala, Sweden) Syro-Wave peptide synthesizer was carried out on a 0.1 mmol scale by the FastMoc methodology, beginning with the Rink Amide MBHA resin (Iris Biotech, Marktredwitz, Germany) (150 mg, loading 0.65 mmol/g). The N^α-acetylation was obtained by use of Ac_2O in the presence of N-diisopropylethylamine (DIPEA). At the end of the synthesis, the peptide was cleaved from the resin, filtered, and collected. The solution was concentrated under a flow of nitrogen, and the residue was treated with a solution of NH_4OH to restore the TOAC free-radical moiety.

The crude peptides were purified by preparative RP-HPLC on a Phenomenex Jupiter C18 column (22 x 250 mm, 10 μ, 300 Å) using a Shimadzu (Kyoto, Japan) LC-8A pump system equipped with a SPD-6A UV-detector (flow rate: 12 mL/min, λ=216 nm) and a binary elution

system: A, 0.05% TFA; B, 0.05% TFA in CH_3CN/H_2O (9: 1 *v/v*); gradient 35-65% B in 40 min. The purified fractions were characterized by analytical RP-HPLC on a Phenomenex Kinetex C18 column (4.6 x 100 mm, 3.5 µ, 100 Å) with an Agilent (Santa Clara, CA) 1200 HPLC system equipped with both UV and MS (Agilent, Quadrupole 6300 LC/MS) detectors. The binary elution system used was as follows: A, 0.05% TFA in H_2O; B, 0.05% TFA in CH_3CN; gradient 35-65% (*v/v*) B in 20 min (flow rate 1 mL/min); spectrophotometric detection at λ=216 nm.

DEER Spectroscopy: Measurements

An X-band Bruker ELEXSYS E580 EPR spectrometer was used. Three-pulse DEER experiments were carried out using a split-ring Bruker ER 4118 X-MS-3 resonator and an Oxford Instruments CF-935 cryostat. The length of pumping pulse was 32 ns, the lengths of the echo-forming detection pulse sequence were 16 and 32 ns, respectively. The amplitude of the pulses was set to provide maximum echo signal in the absence of the pumping pulse. The time delay between two detection pulses was 650 ns. The pumping pulse was scanned with a step of 8 ns, starting at a time delay of 200 ns prior to the first detection pulse. The starting delay T for the DEER time trace analysis ($T = 0$) was determined as described previously,[24] using 5 mM TEMPONE nitroxide in glass solution. The pumping pulse in all cases was applied at the frequency v_B corresponding to the maximum of the echo-detected EPR spectrum, and the difference $v_A - v_B$ between the detection and pumping frequencies was set to 70 MHz. The DEER signal distortion upon the pumping pulse passage through the detecting pulses were corrected as previously described.[25] The resonator was cooled with gaseous nitrogen. The sample temperature was kept near 77 K.

DEER Spectroscopy: Data Analysis

For doubly spin-labeled molecules, the DEER time trace depends on two contributions: the intramolecular one, arising from interactions between two labels in the molecule, and the intermolecular one, arising from interactions between labels in different molecules. These two contributions can be assumed to be independent so that the DEER time trace is obtained as a product:

$$V(T) = V_{INTRA}(T)V_{INTER}(T) \tag{1}$$

The theory predicts that[10,13,26]

$$V_{INTRA}(T) = V_{INTRA}(0)(1 - p_B(1 - f(T))) \tag{2}$$

where the factor p_B is determined by the parameters of the pumping pulse (it characterizes the portion of spins excited), and

$$f(T) = \frac{1}{2}\int_0^\pi \sin\theta d\theta \int_0^\infty \cos(\frac{\gamma^2\hbar}{r^3}(1 - 3\cos^2\theta)T))P(r)dr \tag{3}$$

where $P(r)$ is the distance distribution function between the two spin labels in the molecule. This function is assumed to be normalized, $\int_0^\infty P(r)dr = 1$ (making $f(0) = 1$).

The Fourier transform of the $f(T)$ function

$$F(v) = 2\int_0^\infty f(T)\cos(2\pi vT)dT \tag{4}$$

is a frequency-domain DEER line shape, which can be called as a Pake resonance pattern. Note

that from Eq. (3) it follows that $F(\nu)$ is also normalized, $\int\limits_{-\infty}^{\infty} F(\nu)d\nu = 1$.

$V_{INTER}(T)$ often obeys a simple exponential dependence,

$$V_{INTER}(T) = V_0 \exp(-const \cdot T) \tag{5}$$

The distance distribution function $P(r)$ can be obtained by solving the integral Eq (3). To avoid

instability of solution because of the ill-posed nature of the problem, the solution regularization

is needed.[26] Here, we use two independent regularization approaches: by the distance

discretization with Monte Carlo search of the solution in the DEER frequency domain[27] and

with multi-Gaussian Monte Carlo fitting, also in the frequency domain.[28,29] The Monte Carlo

distance discretization approach is certainly model-free, while the multi-Gaussian Monte Carlo

fitting produces smooth $P(r)$ functions possessing meanwhile a simple physical meaning, and

is widely used as a regularization method in PELDOR/DEER measurements.[28-30]

The Monte Carlo distance discretization approach describe in Ref. 27 was slightly modified in

this work: the trial distribution function $P_{trial}(r_i)$ for the i-th distance point was searched in the

form of $P_{trial}(r_i) = (0.5 - \alpha/2)\xi_{i-1} + \alpha\xi_i + (0.5 - \alpha/2)\xi_{i+1}$ where ξ_i are the random

values generated independently for the i-th distance point and distributed with equal probability

between 0 and 1, and α is a parameter between 0 and 1. It was found empirically that for $\alpha \approx$

0.8 the Monte Carlo search converges much faster than for any other α value.

Circular Dichroism Spectroscopy

CD spectra of the *unlabeled* compounds were obtained using a Jasco J-815 (Tokyo, Japan) spectropolarimeter equipped with a Peltier controlled thermostatic cell. The ellipticity is given as mean residue molar ellipticity, $[\theta]$ (deg cm^2 dmol^{-1}), calculated by Eq. (6):

$$\theta = \frac{\theta_{obs} \cdot MRW}{10 * l * c} \tag{6}$$

where θ_{obs} is the ellipticity in millidegrees, MRW is the mean-residue molecular weight, l is the path length of the cuvette in cm, and c is the peptide concentration in mg mL^{-1}. A 1.0 mm quartz cuvette was used, with a final peptide concentration of 200 μM in PBS (pH = 7.4). Spectra were recorded from 250 nm to 190 nm at 25 °C. Unless stated otherwise, data points were collected with a 0.5 nm interval, with a 1-nm bandwidth and a scan speed of 1 nm per second. Each spectrum was an average of 5 scans. The percentage of α-helicity was calculated using the value $[\theta]_{222} = 40000 \times (1-4.6/n)$,[31] as 100% value for an α-helical peptide of *n* residues. For the analysis, each spectrum had the appropriate background spectrum (buffer or 50% TFE) subtracted.

The CD curves of the *TOAC-labeled peptides* were recorded on a Jasco J-1500 spectropolarimeter equipped with a Haake thermostat (Thermo Fisher Scientific, Waltham, MA). Baselines were corrected by subtracting the solvent contribution. A fused quartz cell of 0.2 mm pathlength (Hellma, Mühlheim, Germany) was employed. Spectrograde TFE 99.9% (Acros Organic, Geel, Belgium) was used as solvent.

RESULTS

Design of the Double-TOAC Labeled, α-Helical Peptides

For a DEER investigation, an appropriate average intramolecular distance between the two nitroxyl free radicals in double-labeled peptides is considered to be in the range 20-25 Å. Since the conformational target of the present study is an α-helical, coiled-coil peptide system, we first took into consideration that 3.6 α-amino acids are involved in a complete turn of this type of helix.[14,15] Therefore, seven α- amino acids ($i \rightarrow i+7$) are needed to place two side chains exactly one on top of the other, thus eliminating the undesired side-chain "orientational effects". The distance between corresponding atoms of two consecutive turns is about 5.5 Å (α-helix pitch). As a consequence, after seven amino acids this separation increases to 11 Å. Thus, to achieve the EPR-desired separation range mentioned above, a sequence of 14 residues (radical probe relative positions $i \rightarrow i+14$) is required. Note that, in a stable α-helix, at least the two N-terminal residues (as well as the two C-terminal residues) are considered rather mobile if compared to the internal residues in the sequence.[32] To sum up, one can safely work with a sequence of at least 20 amino acids to obtain an overall, *internal* rigid EPR ruler. This is the reason why our unlabeled peptides are based on 21 amino acids and selected among the most helicogenic (Ala, Leu, Lys, Glu) residues occurring in proteins. At this point, it was easy for us to decide the most reasonable positions (4 and 18) for the two TOAC incorporations, each replacing a (weaker) helix-supporting Ala residue, while maintaining the functionality of coiled-coil formation.

Peptide Synthesis and Characterization

Standard, solid-phase peptide synthesis (SPPS) protocols, appropriate to the automated synthesizer employed, were used for the synthesis of both the *unlabelled* and *TOAC-containing* peptides. The synthesis of the latter peptides proved to be difficult, due to susceptibility of the

nitroxide radical probe to the acidic conditions required for the peptide cleavage from the resin and the side-chain deprotection procedures. In the presence of TOAC residues, the acidic conditions required for the final cleavage convert the free radical to its N-hydroxylated species.[33-35] The recovery of the nitroxyl radical is obtained through an alkaline treatment with 1 M ammonium hydroxide for 180 minutes. The reaction was checked by HPLC analysis. The complete regeneration of the free radical character was confirmed by EPR spectroscopy.

The correctness of the chemical assignments to the peptide fractions obtained by HPLC purification was confirmed by HPLC-MS analyses (Table S1).

CW EPR and DEER for Homodimerization of K** and Heterodimerization of Its Hybrid (Labeled/Unlabeled) K**/E

CW-EPR spectra of labeled *K*** and its hybrid labeled/unlabeled K**/E samples were recorded at 180 K. All curves are typical of immobilized nitroxides. Selected, representative data are shown in Figure 2 for peptides in different solutions. The helix-promoting solvent TFE is known to disrupt E/K dimers,[1] while PBS is expected to stabilize the heterodimerization. In the case of K** in PBS, a limited line broadening is seen. This effect takes place because of additional magnetic dipole-dipole interactions between spin labels, which in turn may originate from peptide clustering.
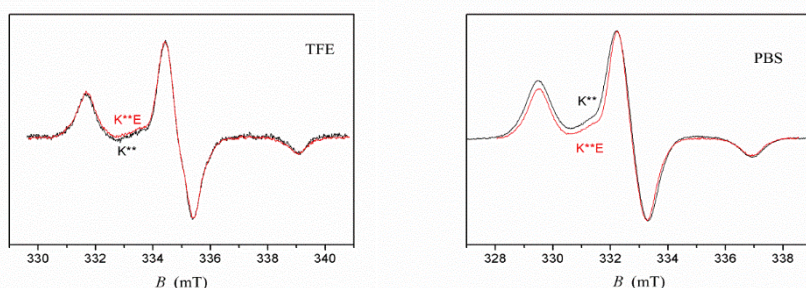

Figure 2. CW-EPR spectra of labeled K** and its hybrid labeled/unlabeled K**/E samples recorded in TFE (left) and PBS (right). For K** in PBS, a modest line broadening is seen.

The DEER time traces of these two samples are shown in Figure 3. The data were obtained from the original $V(T)$ time traces by division on the intermolecular contribution $V_{INTER}(T)$, which results in the $V_{INTRA}(T)$ time traces [Eq. (1)]. $V_{INTER}(T)$ was obtained from the asymptotical behavior of the DEER original data, which were found to be close to the exponential values [Eq. (5)]. The correctness of this $V_{INTER}(T)$ approximation is justified by the asymptotical, horizontal behavior of the resulting $V_{INTRA}(T)$ data (Figure 3, bottom).
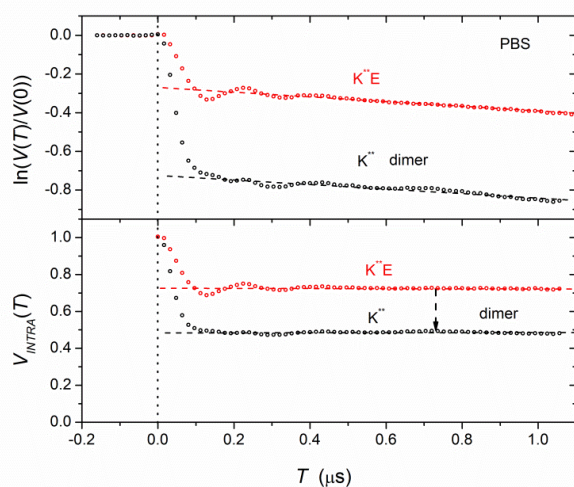

Figure 3. Representative three-pulse DEER time traces shown for the K** (homo-oligomer) and K**/E (heterodimer) peptides in PBS. Top: semi-logarithmic plot of the original $V(T)$ data. Bottom: background-free intermolecular contribution $V_{INTRA}(T)$ obtained by division for the asymptotical exponent. In both cases, dashed lines show an asymptotical linear behavior. The vertical dotted line indicates the zero T position.

Data for the K**/E sample in PBS buffer show a decay and oscillations typical of biradicals.[13] The asymptotical value achieved for this sample is 0.725 ± 0.005. In contrast, the signal of the pure K** sample decays faster and the oscillations become substantially damped to the asymptotical value of 0.48 ± 0.01. The extent of the depth of the plateau has been already reported for self-assembled, *mono*-TOAC labeled peptide molecules to be dependent on the

self-aggregate number.[13] Thus, also for K** the same phenomenon, namely presence of homo-oligomers (dimers, trimers), is seen.

More important is the observation of the higher plateau value seen for K**/E (0.725). Thus, in the presence of unlabeled E, self-aggregation of K** is prevented, due to formation of the thermodynamically more stable K**/E heterodimers. Comparable results were achieved from the CD analysis of the temperature-dependent refolding curves (the binding constants for homo-dimerization of the unlabeled K peptide and for heterodimerization of the unlabeled K/E peptides are K_F (25 °C) 3.42 x 10^3 M^{-1} and K_F 1.77 x 10^7, respectively).[32]

Data for the K**/E sample are transformed into a normalized form:[24]

$$V_N(T) = \frac{V_{INTRA}(T) - V_{INTRA}(\infty)}{V_{INTRA}(0) - V_{INTRA}(\infty)} \tag{7}$$

with the subsequent relation that $V_N(T) = f(T)$, determined by Eq. (3). An example of the $V_N(T)$ obtained is shown in Figure 4 (left). Then, for $V_N(T)$ a cosine Fourier transform was taken, and resulting Pake doublet [inset to Figure 4 (left)] in the frequency domain was fitted with the distance distribution function $P(r)$, employing the Fourier-transformation given by Eq. (4). The was fitting performed using two independent approaches (see subsection DEER Spectroscopy: Data Analysis), namely regularization by the length of distance discretization with Monte Carlo calculations and multi-Gaussian Monte-Carlo fitting. Figure 4 (right) shows that both approaches produced similar results (see also SI, Figures S3, S4).
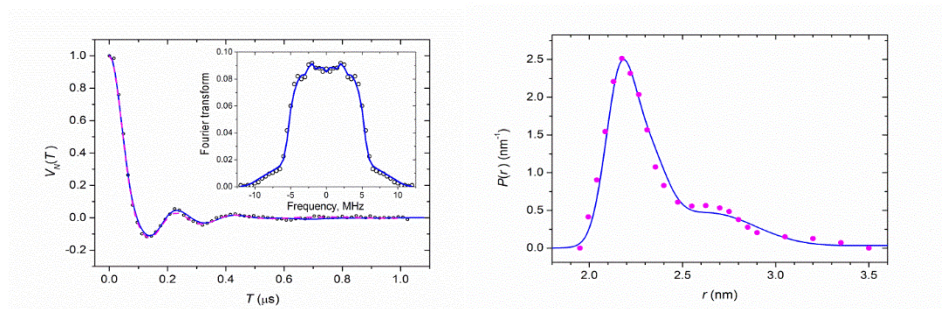

Figure 4. Left: the DEER time trace $V_N(T)$ normalized with Eq. (6) for the K**/E dimer in PBS (empty circles), taken as a mixture of experimental data for two frequency offsets, 70 and 80

MHz (see text) with the results of the multi-Gaussian fitting (solid blue line) and by the fitting based on the regularization using distance discretization (dashed magenta line). The inset shows the Fourier transform (Pake pattern) of the experimental data (empty circles) and of the results of the multi-Gaussian fitting (solid blue line). Right: the distance distribution function obtained using the multi-Gaussian fitting (solid blue line) and by the fitting based on the regularization using distance discretization (magenta circles).

The problem of the orientational selectivity, often taking place in DEER of doubly-spin-labeled molecules,[20] was overcome in this work by comparing the Pake resonance patterns obtained for different observation-pumping frequency offsets (SI, Figure S1). Luckily, for combination of the data for two offsets, 70 and 80 MHz, the Pake pattern was found to correspond to the random relative orientational distribution of the two spin labels (SI, Figure S2).

DEER TOAC[4,18] Distance Distributions for K** and Its Hybrid(Labeled/Unlabeled) K**/E

In Figure 5 the distance distributions $P(r)$ are given for the different samples studied, obtained using the multi-Gaussian Monte-Carlo fitting. First, the distance distribution for the PBS samples will be discussed, because they are relevant for understanding the role of K**, and K**/E in biological experiments. The distance distribution for K** in PBS is not shown, because of the theoretical complexity in the analysis of the four-spin K**/K** system.[36] As we have seen before, this problem does not arise for the K**/E system in PBS. The main peak measured for K**/E exhibits a maximum at 2.17 nm (± 0.06 nm) that agrees with the TOAC[4]•••TOAC[18] distance (2.21 nm) of the α-helical model for the K**-peptide (inset of Figure 1). In addition, a shoulder is shown with a maximum at 2.35 nm.
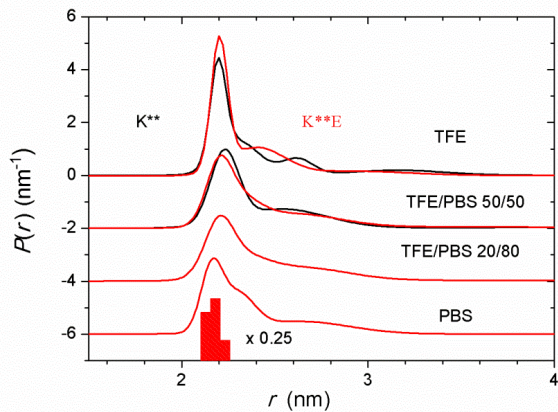
Figure 5. Distance distribution functions obtained with the multi-Gaussian Monte-Carlo fitting for labeled K** in glassy solution (black curves) and its hybrid labeled/unlabeled K**/E (red curves) samples in PBS and at different TFE/PBS ratios. The red histogram shown in the abscissa indicates the NMR distance distribution obtained at ~20% TFE (calculated from the coordinates of the C^{α} atoms of Ala^4 and Ala^{18}, stored into the 1OL – pdb structure) for the unlabeled K peptide associated with the unlabeled E peptide.

Finally, an extremely broad 'wing' is also apparent (the tailing starts from 2.35 nm up to *ca.* 3.2 nm) which might possibly be attributed to multiple contributions of different conformations (see *Discussion* section below). However, we didn't observe any variation in the presence of the unlabeled E molecule.

In 20% TFE, we found one sharp distribution for K** with a maximum at 2.21 nm (±0.05 nm). It should be noted that in this specific case the distance distribution can indeed be calculated because we did not observe any anomalous signal decay, indicating the absence of any homo-oligomerization. Remarkably, this distance distribution coincides with that observed for K**/E (red curve), suggesting that the conformation of K** (the black curve is not visible because of the overlapping red curve) does not change upon association with the unlabeled E in 20% TFE. Evidently, the presence of a small amount of TFE is stabilizing the E/K structure due to a more stable salt bridge between the negatively charged glutamates and positive lysines, located at the *e* and *g* positions shown in the helical diagram (see below in Figure 8).

In this connection, it is important to remember that we have chosen this experimental condition for comparison with the 23% TFE condition used for resolving the NMR 3D-structure.[7] The histogram, indicating the NMR distance distribution calculated from 20 NMR models for the 4-18 segment of the K peptide (associated with E), is illustrated in the abscissa of Figure 5. The NMR distance agrees very well with the DEER distance at 20% TFE, (2.16 nm ± 0.04 nm). Interestingly, the 2.35 nm shoulder observed for K**/E in PBS is not shown in this case. Evidently, the 2.35 nm conformer is not stable. This finding makes clear why 23% TFE/PBS was chosen for resolving the NMR structure.

At 50% TFE, paramagnetic NMR experiments highlighted that the quaternary E/K structure is disrupted.[8] Thus, the curves shown at 50% and 100% TFE should be attributed to isolated helices. Therefore, we don't expect different effects for K** and K**/E. Nevertheless, the main peak appears to be slightly shifted for the TFE conditions shown here, likely due to a modest change of the φ, ψ backbone torsion angles induced by the TFE solvent molecules, while preserving the classical α-helix intramolecular $i+4 \rightarrow i$ C=O•••H-N H-bonding pattern.

At 100% TFE, the minor K** black curve at the distance of 2.62 nm shifts to 2.42 nm upon association with E (red curve). This effect occurs due to the lack of screening of the ionic charges (K** and E peptides exhibit overall charge 3+ and 3-, respectively) in water ($\varepsilon = 80.1$) as compared to that in TFE ($\varepsilon = 8.55$). We believe that K**- and E-ion pairing might cause the change of the 3D-structures, due to the Coulomb interactions between the charged peptides, instead of the hydrophobic (IAAL) interactions, responsible for the stabilization of the coiled-coil system at 20% TFE ($\varepsilon = 72$).[41]

DEER TOAC[4,18] Distance Distributions for E** and Its Hybrid(Labeled/Unlabeled) E**/K

In Figure 6 the distance distributions of E**/K in PBS and its mixture with TFE are given. All samples show similar distance distributions with a maximum at 2.20 nm, independent of the

presence or absence of the unlabeled K, which agrees with both the maximum distance and its spread in the α-helical NMR structure. The conformer at 2.34 nm observed for K**/E in PBS is not seen in this case. Moreover, the TFE-dependent shift of the main peak observed for K**/E at different conditions is not shown in the case of E**/K.

The free peptide E** in PBS exhibits homo-oligomerization, although to a lesser extent than K**.[33] At 20% TFE, E** shows, beside the peak at 2.20 nm, an additional well resolved peak, but at the shorter distance of 1.9 nm, which is likely attributed to a bending or nicking of the helical molecule. Evidently, the free E** peptide is characterized a more flexible conformation than K** under the same condition, while both E** and K** are stabilized by their counter-ion partners.

At 50% TFE, the 1.9 nm peak observed for pure E** shifts to 2.0 nm, while under this condition, for which the E**/K heterodimer is expected to be dissociated,[8] the distance distribution shown for E**/K exhibits a shoulder near the main peak at 2.20 nm. Probably, the dissociation of the heterodimer is not completed under this condition.

Interestingly, at 100% TFE, the E** and E**/K curves don't overlap. In this case, ion pairing of E** with K leads to an extension of the 3D-structures, *i.e.* for pure E**, 2.22 nm and 2.43 nm, while for E**/K, 2.25 and 2.53 nm.
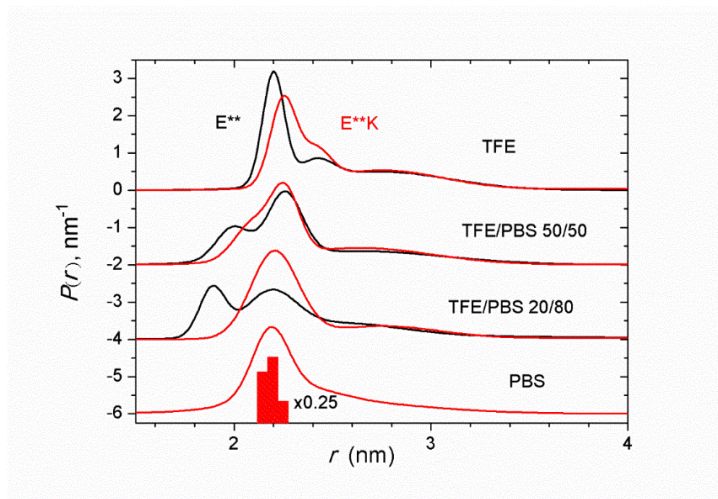
Figure 6. Distance distribution functions obtained with multi-Gaussian Monte-Carlo fitting for labeled E** in glassy solution (black curves) and its hybrid labeled/unlabeled E**/K (red curves) samples in PBS and at different TFE/PBS ratios. For the E**K system in 20/80 (*v/v*) TFE/PBS, the black and red curves practically coincide. The histogram shown in the abscissa illustrates the NMR distance distribution (obtained at ~20% TFE and calculated from the coordinates of the C^α atoms of Ala[4] and Ala[18] for the E peptide (associated with the K peptide in the 1UOL-pdb structure).

CD Spectroscopy Results

In general, all far-UV CD spectra of the *unlabeled* K and E peptides, and of the coiled-coil K/E system as well, show the classical three-band (negative, negative, positive from 250 to 190 nm) shape with approximately comparable intensities characteristic of a well-developed, right-handed, α-helical conformation. The Cotton effect at about 222 nm is assigned to the n→π* transition of the backbone amide chromophores, while those at approximately 208 and 192 nm are attributed to the parallel and antiparallel components of the π→π* transition of the same chromophores in a helical arrangement.

Figure 7A illustrates the CD spectra recorded in PBS. The results agree with those previously reported.[1] The amounts of helical structure present in the molecules, calculated from the $[\theta]_{222}$ ellipticity values, are given in Table 2. Thus, the K peptide exhibits a rather limited percentage (40%) of ordered conformation, which however is largely stabilized (to 86%) in the presence

of E by coiled-coil formation. For the E peptide, the percentage of helicity (25%) was found to be lower than that of K. It should be noted that the $[\theta]_{222}/[\theta]_{208}$ ratios for K (0.86) and E (0.71) increase to 1.16 for K/E, indicating in the latter the presence of a heterodimer. These findings confirm those from published sedimentation equilibrium experiments.[1]
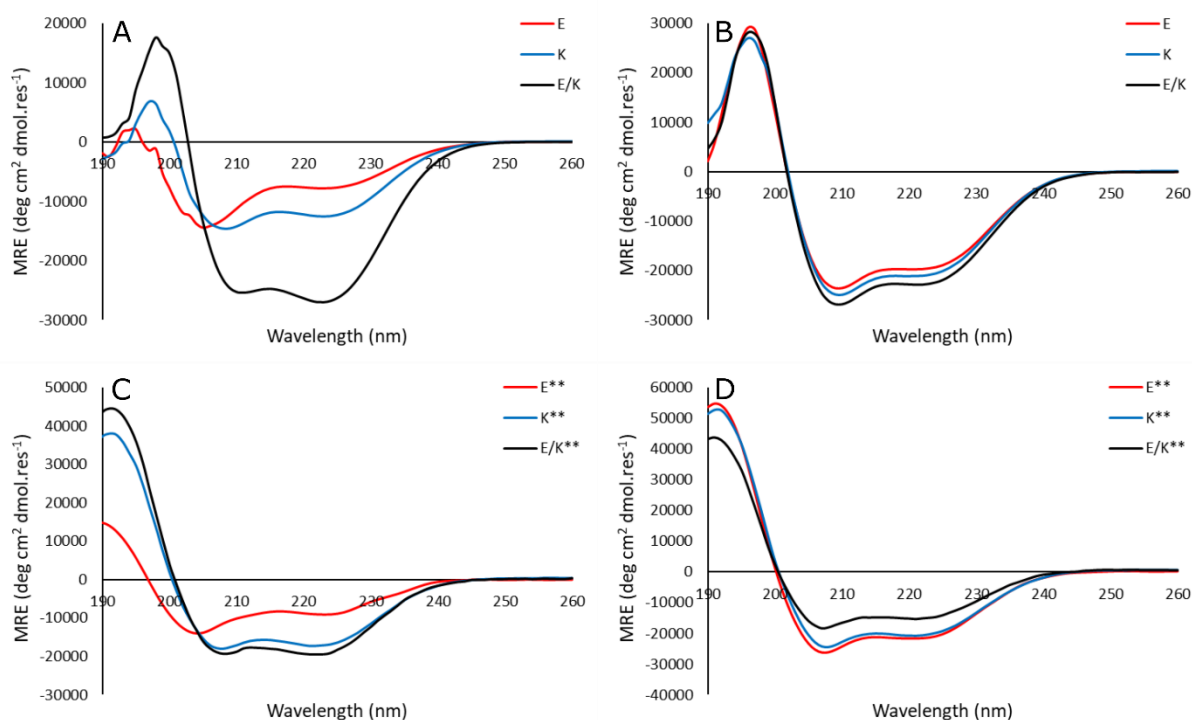

Figure 7. (A) CD spectra for K, E, and for the equimolar mixture K/E in PBS: [total peptide]= 200 μM, 25°C; (B) CD spectra for K, E, and for the equimolar mixture K/E in 50% TFE: [total peptide]= 200 μM, 25°C; (C) CD spectra for K**, E**, and for the equimolar mixture K**/E in PBS: [total peptide]= 200μM, 25°C; (D) CD spectra for K**, E** and for the equimolar mixture K**/E in 50% TFE: [total peptide] = 200 μM, 25°C.

Table 2

Helicity (%)[a]	PBS	20% TFE	50% TFE	100% TFE
K	40	67	68	53
E	25	61	63	58

K**	54	60	66	66
E**	29	60	69	69
K / E	86	72	73	55
K** / E	61	46	48	47

^aCalculated from the $[\theta]_{222}$ ellipticity value.[29]

Addition of 20% TFE to PBS increases remarkably the amounts of helical structures for both peptides K (67%) and E (61%) (Table 2). These values remain essentially unchanged at 50% TFE (68% and 63%, respectively) (Figure 7B), clearly suggesting that ordered secondary structure formation between 0% and 50% TFE in these compounds is not a gradual process. However, they experience a limited decrease (53% and 58%, respectively) in 100% TFE. It is worth mentioning, however, that adding any TFE percentage greatly deteriorates the stability of the K/E coiled-coil system (72, 73, 55 %, respectively).

Figures 7C and 7D show the CD spectra of the *double-TOAC labeled* K** and E** peptides, and of the coiled-coil K**/E system in PBS and 50% TFE, respectively. Importantly, for sufficiently long (more than six residues), right-handed α-/3_{10}-helical peptides the contribution by the (weak) induced CD of the TOAC *side-chain* aminoxyl (NO) $\pi{\rightarrow}\pi^*$ transition is not dominating the region of the peptide chromophore, thereby not precluding any identification of the backbone conformation adopted.[37]

As expected from the known, higher helical propensity of TOAC *versus* Ala, in PBS the K** helicity (54%) is significantly higher than that of its unlabeled K counterpart (40%) (Table 2). This conformational tendency is also found for E (25%) *versus* E** (29%), but quantitatively it is much less remarkable. In any case, this difference tends to level off as 20% and 50% TFE are added to the PBS solution, where all four double-TOAC labeled/unlabeled compounds are characterized by almost equal, quantitatively much more relevant values (60-69%).

23

Interestingly, however, in pure TFE the same phenomenon seen for the unlabeled K and E peptides, namely that helix percentages (53-58%) are lower than at 50%TFE (63-68%) does not take place, remaining essentially the same (66-69%).

The CD properties of the K**/E mixture in PBS support the view that the already relevant percentage (54%) of helicity characterizing the double-TOAC labeled K** molecules does indeed increase, but only to a rather modest extent (61%), in the mixed K**/unlabeled E coiled-coil system (Table 2). Moreover, by adding different amounts of TFE to the latter in PBS, not only a similar, marked decrease in its coiled-coil stability (46-48%) is observed, as for K/E, but even for the percentages of ordered conformation seen for K** (60-66%) and E (60-69%) separately. As previously recorded for the unlabeled K/E coiled-coil system in PBS (Figure 7A), also for the K** labeled, corresponding K**/E system in the same environment (Figure 7C) the $[\theta]_{222}/[\theta]_{208}$ ratio (a CD probe for heterodimer formation) increases, albeit slightly, to a value greater than 1.00.

DISCUSSION

DEER Spectroscopy as a Tool for Investigating Peptide Conformation

In this study, DEER spectroscopy applied to intramolecular double-TOAC labeling allowed us to describe the conformation of the 4-18 segment of K**, E**, K**/E and E**/K, with site-specifically replacing Ala residues at well-chosen positions of the peptide backbone. Under almost all conditions, the distance distributions observed for K**/E (2.17 ± 0.06 nm) and E**/K (2.18 nm) perfectly agree with pure α-helical structures, as shown from the Hyperchem model and NMR structures (Figure 1). The spread of the measured distance distribution is remarkably small, corresponding to rather stiff 3D-structures. However, one does not expect to find the same conformational purity for the free peptides K** and E** under most of the conditions studied. Only K** associated to unlabeled E is shown not to be a classic α-helix in PBS, as

suggested by the conformer at 2.43 nm. We attribute this latter peak to a superhelix involving the E helix. Note that this conformer is not observed for E**/K. Probably, the K** helical molecule might be wrapping around the long axis of the E-helix, thereby slightly extending the distance (0.17 nm) of K** between the two labels. Thus, if this hypothesis would be correct, K** wraps around E, but not *vice versa*. The absence of the 2.43 nm peak for K**/E in 20% TFE indicates that the proposed supercoil is destabilized under this condition, thus explaining why 23% TFE has been reported as the optimal percentage for resolving the E/K NMR 3D-structure.[7] In pure PBS the NMR spectrum reveals severe line broadening, preventing one from assigning the signals to specific protons of the molecule. This line broadening was suggested to be caused by non-specified quaternary interactions of the subunits forming a higher molecular weight multimer at the higher concentrations used for NMR. DEER generally supports this view, but it also exhibits a more specific conformation for K**/E (2.34 nm), which is shown to be stable in pure PBS, but unstable in 20% TFE. Finally, DEER excludes the possibility of mixtures of the α-helix and the longer 3_{10}-helical structure, that would be otherwise difficult to detect from NMR data.

The repetitive nature of the heptad comprising the sequences of the two subunits in the complex, and consequently the high degree of chemical shift redundancy, makes resolving the E/K system by NMR difficult. This problem was overcome by using a combination of ^{1}H-NOE restraints and the homology structure of the *c*-June coiled-coil homo-dimer.[38] From the conformational point of view, the present DEER study agrees with this 3D-structure.

K** Forms Homodimers, while K**/E Forms Heterodimers under the Same PBS Condition

The phenomenon of an initially recorded fast drop of the signal decay, eventually leading to a relative low plateau of the signal amplitude, is a typical characteristic for the presence of aggregates. From the extent of the depth of the plateau, the number of molecules involved in

the aggregates can be estimated as already reported for the *self*-assembled *mono*-TOAC labeled trichogin GA IV in non-polar solutions.[15] A similar phenomenon was published for the ^{19}F-^{19}F CODEX solid-state NMR of self-assembling ^{19}F-labeled peptides.[39-41]. Although the range of distances between the ^{19}F probes is rather short (about 10 Å), it falls close to the silent range of DEER detection (about 15-80 Å).

In this work, we observed the same anomalous signal decay, but for a double labeled cationic $(K^{**})_2$ dimer in PBS (Figure 3). In the presence of non-labeled E, however, the peculiarities of the signal decay appeared as usually observed for a biradical. It is evident here that the dimer is disrupted, thereby yielding the self-recognizing coiled coil K**/E system. This biradical allows us to measure the distance distribution between residues 4 and 18 of the individual K** in its assembled state and its conformation in PBS as well. We are wondering why the α-helical conformation remains stable in the NMR-conditions 20/80 (*v/v*) TFE/PBS, as TFE is known to disrupt quaternary structures. The helical diagram, shown in Figure 8, may help to rationalize the homodimer to heterodimer conversion and answer this question about the role of TFE in the stabilization of the coiled coil. Note that both quaternary structures adopt parallel associated helices.[11]
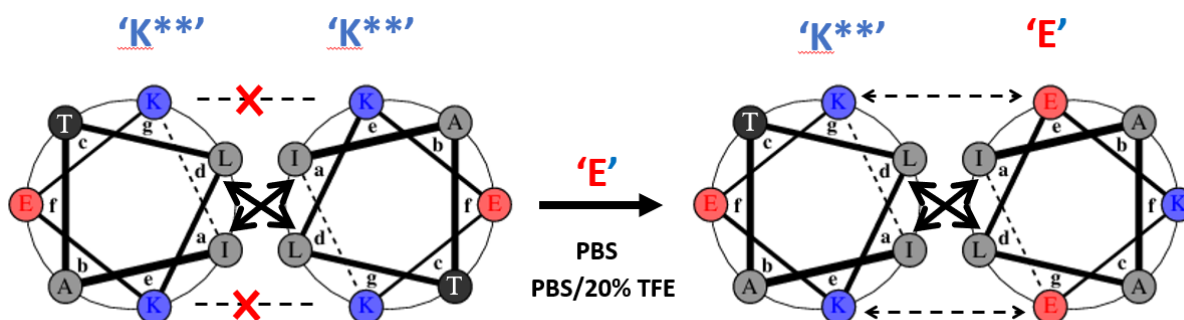
Figure 8: Helical diagram showing the different distributions of ionic amino acid side chains of homo- (left) and hetero- (right) dimer. Positively charged K and negatively charged E are colored blue and red, respectively. For clarity, only C-terminal heptad fragments are shown for K** ($I^{15}AT^{18}LKEK$) and E ($I^{15}AALEKE$). All helices are viewed perpendicularly oriented to the page and directed from the N- to the C-terminus. The packing of inter helical associated hydrophobic side chains of I and L are indicated by black arrows. Salt bridges at the *e* and *g* positions of the heterodimer are shown by dashed lines.

It is generally accepted that the main driving force for E and K association in PBS is caused by hydrophobic interactions of branched I and L residues, minimizing their unfavorable interaction with water molecules. In addition, salt bridges between E- and K- amino acids are assumed also to stabilize the structure. The diagram also explains the relative lower thermodynamic stability of the dimer.[33] Thus, Coulomb interactions are suggested to play an important role, which may be partly weakened by screening effects of the surrounding water dipoles and the salt ions Na^+/Cl^- constituting the buffer PBS ($\varepsilon = 80$). Thus addition of 20% TFE to PBS ($\varepsilon = 72$)[42] would increase the effects of Coulomb interactions to further stabilize the E/K structure.

A Combined View from DEER and CD Conformational Data

Concerning the support given by CD to DEER spectroscopy, it is important to stress the point that the DEER analysis of double-labeled K** (and E**) peptides is restricted to only 70% (segment 4-18) of the 21-amino acid sequence, thus leaving a significant part of conformational information out of view. It is also important to keep in mind that DEER and CD are based on

totally different physical phenomena, *i.e.* intramolecularly dipolar electron•••electron spin interactions *versus* n→π*/ π →π*amide chromophore ellipticities in the far-UV absorption region, respectively.[43] CD records the average percentages of the helices, sheets and the so-called 'random coil' conformations, while DEER determines the distance distribution between TOAC labels for K** (or E**), with and without being assembled with their unlabeled peptide counterparts. Spectral overlap of the contributions from α- and 3_{10}-helices, and β-conformations are difficult to be specifically distinguished by CD, while DEER allows one to observe them separately by their distinct distance distributions.

Helix Propensies Calculated from CD and DEER Data

The helix propensies calculated for K and K/E in PBS amount to 40% and 86%, respectively. However, these values calculated from CD-derived empirical formulas are not expected *a priori* to match the DEER data. The CD remaining fractions, 60% and 14% respectively, usually represent mixtures of conformations, *i.e.* the 'random coils' (a statistically distribution of partially folded structures) and the multitude of conformations generally described by the 'gyration model.[44] The broad wing (*ca*. 30 % of the total integral) shown in the DEER distance distribution functions likely agree with the gyration model. However, random coils would possibly fall outside the range of DEER detection (TOAC4•••TOAC18 < 1.5nm). Since it is not clear whether the DEER 2.34 nm fraction would contribute to the CD spectra or not, this uncertainty makes a quantitative analysis questionable.

Nevertheless, DEER and CD data are consistent about the relative different helical stabilities of the single helices (K > E) observed in different PBS/TFE conditions. On the first sight, this observation would be surprising because of the similar design of their peptide sequences, but differs with respect to the charged side chains. The diverging nature of the E and K peptides has been also experimentally observed by their different affinities to zwitterionic lipid

membranes.[45] From the present observations this divergence is likely due to intrinsic different properties of the peptides, exhibited by different Coulomb repulsions of the amino acid side chains. The side chains of the negatively charged Glu residues would affect the helix stability because they are separated from the helix backbone by only two carbons, while the positive side-chain charges of Lys are separated by four carbon atoms.

CD and DEER about the TFE Effect

The most established effect of TFE in CD studies of peptides is its ability to promote helical structures mainly due to dehydration of the C=O•••H-N H-bonds, accompanied by disruption of a network of water molecules in a chaotic manner. In many CD studies, the effect of helix induction by TFE levels off at *ca.* 50 %.[29] A recent molecular dynamics study suggests the formation of clusters around the peptides.[46]

The DEER small distance shift (1.71-2.21 nm) of the narrow lines observed for K** at different TFE concentrations certainly cannot be explained by the presence of conformational mixtures. Most likely, the shifts should be attributed to small changes of the φ, ψ backbone torsion angles of the helical molecule due to the energy stabilizing effects of the surrounding TFE molecules. Interestingly, the TFE-dependent shifts are not found for the E** and E**/K peptides. Evidently, the different side chains of E and K molecules are playing a relevant role during their interactions with the solvent TFE molecules. The ionic nature of the sequences is highlighted by DEER at 100% TFE and is likely correlated with the blue shift of the $\pi \rightarrow \pi^*$ band below 200 nm of the CD spectrum recorded for K/E under this condition.

Would the Approach of Double TOAC-Nitroxide Labeling Be Suitable for Pharmaceutical Research of Protein Antagonists, Hormones and Enzyme Ligands?

There are three keys to answer this question: (i) The double TOAC-nitroxide labeling ensures DEER signal detection without any environmental distortion. (ii) The conformation of interest would certainly be a specific one (conformational mixtures and averages of them are not playing any remarkable role). (iii) The standard conformations considered here would not necessarily be at their lowest free-energy states, as has been tested in our present study. Thus, it would be necessary to combine the DEER double-labeling method with distance-restrained molecular dynamics simulations.

Nevertheless, the present combined DEER/TOAC approach has been shown to be extremely accurate and reliable, and fulfil the target conditions for further conformational investigations of more complex biological systems.

CONCLUSIONS

The obtained results show that combining DEER/TOAC analysis with double-TOAC labeling provides extremely precise conformational information (without any modeling), particularly from distance distributions between the well-defined unpaired nitroxide oxygen atoms, on a peptide coiled-coil system independent from its molecular environment. The DEER conformational information agrees with both NMR and CD data.

As a regularization method to solve the ill-posed problem in deriving the $P(r)$ distribution function, the combination of two independent regularization approaches was used here. The first one employs the regularization by optimizing the distance discretization length, while the second one is based on multi-Gaussian fitting. Both approaches use Monte Carlo calculations in the DEER frequency domain (the Pake resonance pattern). The first approach is model-free, while the second approach produces smooth $P(r)$ distributions. The robustness of this combined method can be readily checked not only by agreement with the experimental DEER time traces but also by coincidence of the $P(r)$ distributions obtained in these two approaches.

A supercoiled structure is herein proposed, characterized by a narrow spread of distance of 2.34 nm, that disappears at 20% TFE. It also explains why the reported NMR 3D-structure could be resolved at 23% TFE, but not in PBS. Under this condition, the coiled-coil is likely stabilized by a salt bridge between the positive and negative charged Lys and Glu at the *e* and *g* positions of the helical wheels of K and E, respectively.

From the large DEER modulation depth in PBS, K** was shown to form oligomers, at variance with the system K**/E, indicating the conversion of homo-oligomers to coiled-coil heterodimers by the stabilizing presence of the (unlabeled) E molecules.

The TFE environment of the K peptides leads to small variations of the ϕ, ψ backbone torsion angles, while maintaining the pure rigid α-helical conformation.

The DEER/TOAC combination described in this article for the conformational analysis of E and K peptides is foreseen as an important inspiration for pharmaceutical research of *quasi*-rigid double-labeled receptor antagonists, hormones, and enzyme ligands.

REFERENCES

1.   Litowski, J. R.; Hodges, R. S., Designing heterodimeric two-stranded α-helical coiled-coils: effects of hydrophobicity and α-helical propensity on protein folding, stability, and specificity. *J. Biol. Chem.* **2002,** *277* (40), 37272-37279.

2.   Reinhardt, U.; Lotze, J.; Zernia, S.; Morl, K.; Beck-Sickinger, A. G.; Seitz, O., Peptide-templated acyl transfer: a chemical method for the labeling of membrane proteins on live cells. *Angew. Chem.-Int. Edit.* **2014,** *53* (38), 10237-10241.

3.   Arya, S. K.; Kongsuphol, P.; Wong, C. C.; Polla, L. J.; Park, M. K., Label free biosensor for sensitive human influenza virus hemagglutinin specific antibody detection using coiled-coil peptide modified microelectrode array based platform. *Sensor Actuat B-Chem* **2014,** *194*, 127-133.

4.   Robson Marsden, H.; Elbers, N. A.; Bomans, P. H. H.; Sommerdijk, N. A. J. M.; Kros, A., A reduced SNARE model for membrane fusion. *Angew. Chem.-Int. Edit.* **2009,** *48* (13), 2330-2333.

5.   Versluis, F.; Voskuhl, J.; van Kolck, B.; Zope, H.; Bremmer, M.; Albregtse, T.; Kros, A., In situ modification of plain liposomes with lipidated coiled coil forming peptides induces membrane fusion. *J. Am. Chem. Soc.* **2013,** *135* (21), 8057-8062.

6.   Yang, J.; Shimada, Y.; Olsthoorn, R. C. L.; Snaar-Jagalska, B. E.; Spaink, H. P.; Kros, A., Application of coiled coil peptides in liposomal anticancer drug delivery using a zebrafish xenograft model. *ACS Nano* **2016,** *10* (8), 7428-7435.

7.   Lindhout, D. A.; Litowski, J. R.; Mercier, P.; Hodges, R. S.; Sykes, B. D., NMR solution structure of a highly stable de novo heterodimeric coiled-coil. *Biopolymers* **2004,** *75* (5), 367-375.

8.   Zheng, T. T.; Boyle, A.; Robson Marsden, H.; Valdink, D.; Martelli, G.; Raap, J.; Kros, A., Probing coiled-coil assembly by paramagnetic NMR spectroscopy. *Org. Biomol. Chem.* **2015,** *13* (4), 1159-1168.

9.   Hanson, P.; Millhauser, G.; Formaggio, F.; Crisma, M.; Toniolo, C., ESR characterization of hexameric, helical peptides using double TOAC spin labeling. *J. Am. Chem. Soc.* **1996,** *118* (32), 7618-7625.

10.   (a) Milov, A.D.; Salikhov, K.M.; Shchirov, M.D., Use of the double resonance in electron spin echo method for the study of paramagnetic center spatial distribution in solids, *Soviet Physics Solid State*, **1981**, *23*, 565–569.

(b) Milov, A. D.; Ponomarev, A. B.; Tsvetkov, Y. D., Electron-electron double resonance in electron spin echo: Model biradical systems and the sensitized photolysis of decalin, *Chem. Phys. Letters*, **1984**, *110* (1), 67–72.

(c) Pannier, M.; Veit, S.; Godt, A.; Jeschke, G.; Spiess, H. W., Dead-time free measurement of dipole-dipole interactions between electron spins. *J. Magn. Reson.* **2000,** *142* (2), 331-340.

(d) Selmke, B.; Borbat, P.P.; Nickolaus, C.; Varadarajan, R.; Freed, J.H.; Trommer, W.E., Open and closed form of maltose binding protein in its native and molten globule state as studied by electron paramagnetic resonance spectroscopy, *Biochemistry* **2018**, *57* (38), 5507-5512 .

11.   Kumar, P.; van Son, M.; Zheng, T. T.; Valdink, D.; Raap, J.; Kros, A.; Huber, M., Coiled-coil formation of the membrane-fusion K/E peptides viewed by electron paramagnetic resonance. *PLoS One* **2018,** *13* (1), e0191197.

12.   (a) Biondi, B.; Peggion, C.; De Zotti, M.; Pignaffo, C.; Dalzini, A.; Bortolus, M.; Oancea, S.; Hilma, G.; Bortolotti, A.; Stella, L.; Pedersen, J. Z.; Syryamina, V. N.; Tsvetkov, Y. D.; Dzuba, S. A.; Toniolo, C.; Formaggio, F., Conformational properties, membrane interaction, and antibacterial activity of the peptaibiotic chalciporin A. Multitechnique

spectroscopic and biophysical investigations on the natural compound and labeled analogs. *Pept. Sci.* **2018,** *110* (5), e23083.

(b) Her, C.; Thompson, A. R.; Karim, C. B.; Thomas, D. D., Structural dynamics of calmodulin-ryanodine receptor interactions: electron paramagnetic resonance using stereospecific spin labels. *Sci Rep* **2018,** *8* (1), 10681.

(c) Mayo, D. J.; Sahu, I. D.; Lorigan, G. A., Assessing topology and surface orientation of an antimicrobial peptide magainin 2 using mechanically aligned bilayers and electron paramagnetic resonance spectroscopy. *Chem. Phys. Lipids* **2018,** *213*, 124-130.

(d) Roser, P.; Schmidt, M. J.; Drescher, M.; Summerer, D., Site-directed spin labeling of proteins for distance measurements in vitro and in cells. *Org. Biomol. Chem.* **2016,** *14* (24), 5468-5476.

13.   Milov, A. D.; Tsvetkov, Y. D.; Raap, J.; De Zotti, M.; Formaggio, F.; Toniolo, C., Conformation, self-aggregation, and membrane interaction of peptaibols as studied by pulsed electron double resonance spectroscopy. *Biopolymers* **2016,** *106* (1), 6-24.

14. Ramachandran, G. N.; Ramakrishnan, C.; Sasisekharan, V., Stereochemistry of polypeptide chain configurations. *J. Mol. Biol.* **1963,** *7* (1), 95-99.

15.   Pauling, L.; Corey, R. B.; Branson, H. R., The structure of proteins: two hydrogen-bonded helical configurations of the polypeptide chain. *Proc. Natl. Acad. Sci. U. S. A.* **1951,** *37* (4), 205-211.

16.   Milov, A. D.; Tsvetkov, Y. D.; Formaggio, F.; Crisma, M.; Toniolo, C.; Raap, J., Self-assembling properties of membrane-modifying peptides studied by PELDOR and CW-ESR spectroscopies. *J. Am. Chem. Soc.* **2000,** *122* (16), 3843-3848.

17.   Milov, A. D.; Tsvetkov, Y. D.; Formaggio, F.; Crisma, M.; Toniolo, C.; Raap, J., The secondary structure of a membrane-modifying peptide in a supramolecular assembly studied by DEER and CW-ESR spectroscopies. *J. Am. Chem. Soc.* **2001,** *123* (16), 3784-3789.

18. Syryamina, V. N. ; Samoilova, R. I. ; Tsvetkov, Yu. D. ; Ischenko, A. V.; De Zotti, M. ; Gobbo, M. ; Toniolo, C. ; Formaggio, F. ; Dzuba, S. A., Peptides on the surface: spin-label EPR and PELDOR study of adsorption of the antimicrobial peptides trichogin GA IV and ampullosporin A on the silica nanoparticles, *Appl. Magn. Reson*. **2016**, *47* (3) 309-320.

19. Milov, A.D.; Samoilova, R.I.; Tsvetkov, Y.D.; De Zotti, M.; Toniolo, C.; Raap, J., PELDOR Conformational analysis of *bis*-labeled alamethicin aggregated in phospholipid vesicles, *J. Phys. Chem. B* **2008**, *112* (43), 13469-13472.

20.   (a) Abdullin, D.; Hagelueken, G.; Hunter, R. I.; Smith, G. M.; Schiemann, O., Geometric model-based fitting algorithm for orientation-selective PELDOR data. *Mol. Phys.* **2015,** *113* (6), 544-560.

(b) Abe, C.; Klose, D.; Dietrich, F.; Ziegler, W. H.; Polyhach, Y.; Jeschke, G.; Steinhoff, H. J., Orientation selective DEER measurements on vinculin tail at X-band frequencies reveal spin label orientations. *J. Magn. Reson.* **2012,** *216*, 53-61.

(c) Polyhach, Y.; Godt, A.; Bauer, C.; Jeschke, G., Spin pair geometry revealed by high-field DEER in the presence of conformational distributions. *J. Magn. Reson.* **2007,** *185*, 118-29.

21.   Milov, A. D.; Samoilova, M. I.; Tsvetkov, Y. D.; Jost, M.; Peggion, C.; Formaggio, F.; Crisma, M.; Toniolo, C.; Handgraaf, J. W.; Raap, J., Supramolecular structure of self-assembling alamethicin analog studied by ESR and PELDOR. *Chem. Biodivers.* **2007,** *4* (6), 1275-1298.

22. Allinger, N. L., Conformational analysis. 130. MM2. A hydrocarbon force field utilizing V1 and V2 torsional terms. *J. Am. Chem. Soc*., **1977** (25), 8127–8134,

23. Raap, J.; van Boom, J. H.; van Lieshout, H. C.; Haasnoot, C. A. G**.,** Conformations of methyl 2'-deoxy-*α*-D-ribofuranoside and methyl 2'-deoxy-*β*-D-ribofuranoside. A proton magnetic resonance spectroscopy and molecular mechanics study. *J. Am. Chem. Soc*, **1988**, *110* (9), 2736-2743.

24.   Kuznetsov, N. A.; Milov, A. D.; Koval, V. V.; Samoilova, R. I.; Grishin, Y. A.; Knorre, D. G.; Tsvetkov, Y. D.; Fedorova, O. S.; Dzuba, S. A., PELDOR study of conformations of double-spin-labeled, single- and double-stranded DNA with non-nucleotide inserts. *Phys. Chem. Chem. Phys.* **2009,** *11* (31), 6826-6832.

25. Milov, A. D.; Grishin, Y. A.; Dzuba, S. A.; Tsvetkov, Y. D., Effect of pumping pulse duration on echo signal amplitude in four-pulse DEER. *Appl. Magn. Reson.* **2011,** *41* (1), 59-67.

26.   Jeschke, G.; Chechik, V.; Ionita, P.; Godt, A.; Zimmermann, H.; Banham, J.; Timmel, C. R.; Hilger, D.; Jung, H., DEER analysis 2006: a comprehensive software package for analyzing pulsed ELDOR data. *Appl. Magn. Reson.* **2006,** *30* (3-4), 473-498.

27.   Dzuba, S. A., The determination of pair-distance distribution by double electron-electron resonance: regularization by the length of distance discretization with Monte Carlo calculations. *J. Magn. Reson.* **2016,** *269*, 113-119.

28. Matveeva, A. G.; Yushkova, Y. V.; Morozov, S. V.; Grygor'ev, I. A.; Dzuba, S. A., Multi-Gaussian Monte Carlo analysis of PELDOR data in the frequency domain. *Z. Phys. Chem.* **2017,** *231* (3), 671-688.

29. Kuznetsova, A.A.; Matveeva, A.G.; Milov, A.D.; Vorobjev, Y.N.; Dzuba, S.A.; Fedorova, O.S.; Kuznetsov, N.A., Substrate specificity of human apurinic/apyrimidinic endonuclease APE1 in the nucleotide incision repair pathway. *Nucleic Acids Res.* **2018**, *46* (21), 11454-11465.

30. (a)Pannier, M.; Schädler, V.; Schöps, M. ; Wiesner, U. ; Jeschke, G.; Spiess, H. W., Determination of ion cluster sizes and cluster-to-cluster distances in ionomers by four-pulse double electron electron resonance spectroscopy. *Macromolecules* **2000**, *33* (21)*,* 7812-7818. (b) Stein, R. A.; Beth, A. H.; Hustedt, E. J., A Straightforward approach to the analysis of double electron–electron resonance data. *Methods Enzymol*. **2015**, *563*, 531–567.

(c) Brandon, S.; Beth, A. H.; Hustedt, E. J., The global analysis of DEER data. *J. Magn. Reson.* **2012**, *218*, 93–104.

(d) Sweger, S. R.; Pribitzer, S.; Stoll, S., Bayesian probabilistic analysis of DEER spectroscopy data using parametric distance distribution models. *J. Phys. Chem. A* **2020**, *124* (30), 6193-6202

31.   Gans, P. J.; Lyu, P. C.; Manning, M. C.; Woody, R. W.; Kallenbach, N. R., The helix-coil transition in heterogeneous peptides with specific side-chain interactions: theory and comparison with CD spectral data. *Biopolymers* **1991,** *31* (13), 1605-1614.

32.   Rabe, M.; Boyle, A.; Zope, H. R.; Versluis, F.; Kros, A., Determination of oligomeric states of peptide complexes using thermal unfolding curves. *Biopolymers* **2015,** *104* (2), 65-72.

33.   Formaggio, F.; Broxterman, Q. B. ; Toniolo, C., Synthesis of peptides based on C^a-tetrasubstituted α-amino acids. In *Houben‑Weyl: Methods of Organic Chemistry,* Goodman, M.; Felix, A.; Moroder, L.;   Toniolo, C., Eds., Thieme: Stuttgart, Germany, 2003; Vol. E22c, pp 292-310.

34.   Marchetto, R.; Schreier, S.; Nakaie, C. R., A novel spin-labeled amino-acid derivative for use in peptide-synthesis: (9-fluorenylmethyloxycarbonyl)-2,2,6,6-tetramethylpiperidine-N-oxyl-4-amino-4-carboxylic acid. *J. Am. Chem. Soc.* **1993,** *115* (23), 11042-11043.

35.   Martin, L.; Ivancich, A.; Vita, C.; Formaggio, F.; Toniolo, C., Solid-phase synthesis of peptides containing the spin-labeled 2,2,6,6-tetramethylpiperidine-1-oxyl-4-amino-4-carboxylic acid (TOAC). *J. Pept. Res.* **2001,** *58* (5), 424-432.

36.   von Hagens, T.; Polyhach, Y.; Sajid, M.; Godt, A.; Jeschke, G., Suppression of ghost distances in multiple-spin double electron-electron resonance. *Phys. Chem. Chem. Phys.* **2013,** *15* (16), 5854-5866.

37.   Bui, T. T. T.; Formaggio, F.; Crisma, M.; Monaco, V.; Toniolo, C.; Hussain, R.; Siligardi, G., TOAC: a useful $C^α$-tetrasubstituted α-amino acid for peptide conformational

analysis by CD spectroscopy in the visible region. Part I. *J. Chem. Soc., Perkin Trans. 2* **2000,** (5), 1043-1046.

38.   Junius, F. K.; O' Donoghue, S. I.; Nilges, M.; Weiss, A. S.; King, G. F., High resolution NMR solution structure of the leucine zipper domain of the *c*-Jun homodimer. *J. Biol. Chem.* **1996,** *271* (23), 13663-13667.

39.   Li, W. B.; McDermott, A., Investigation of slow molecular dynamics using R-CODEX. *J. Magn. Reson.* **2012,** *222*, 74-80.

40.   Salnikov, E. S.; De Zotti, M.; Bobone, S.; Mazzuca, C.; Raya, J.; Siano, A. S.; Peggion, C.; Toniolo, C.; Stella, L.; Bechinger, B., Trichogin GA IV alignment and oligomerization in phospholipid bilayers. *ChemBioChem* **2019,** *20* (16), 2141-2150.

41.   Salnikov, E. S.; Raya, J.; De Zotti, M.; Zaitseva, E.; Peggion, C.; Ballano, G.; Toniolo, C.; Raap, J.; Bechinger, B., Alamethicin supramolecular organization in lipid membranes from 19F solid-state NMR. *Biophys. J.* **2016,** *111* (11), 2450-2459.

42.   Gente, G.; La Mesa, C., Water-trifluoroethanol mixtures: Some physicochemical properties. *J. Solution Chem.* **2000,** *29* (11), 1159-1172.

43.   Woody, R. W., Circular dichroism. *Methods Enzymol.* **1995,** *246*, 34-71.

44.   Cantor, R. S., Schimmel, P.R., The behavior of biological macromolecules. In *Biophysical Chemistry, part III*, Freeman: New York, N.Y.,1980, pp 979-1018.

45.   Rabe, M.; Aisenbrey, C.; Pluhackova, K.; de Wert, V.; Boyle, A. L.; Bruggeman, D. F.; Kirsch, S. A.; Bockmann, R. A.; Kros, A.; Raap, J.; Bechinger, B., A coiled-coil peptide shaping lipid bilayers upon fusion. *Biophys. J.* **2016,** *111* (10), 2162-2175.

46.   Vymetal, J.; Bednarova, L.; Vondrasek, J., Effect of TFE on the helical content of AK17 and HAL-1 peptides: theoretical insights into the mechanism of helix stabilization. *J. Phys. Chem. B* **2016,** *120* (6), 1048-1059.

Graphical Abstract TOC